



Title	Morphological and functional analyses of adult onset vitelliform macular dystrophy.
Author(s)	Saito, W.; Yamamoto, S.; Hayashi, M.; Ogata, K.
Citation	British Journal of Ophthalmology, 87(6), 758-762 https://doi.org/10.1136/bjo.87.6.758
Issue Date	2003-06
Doc URL	http://hdl.handle.net/2115/20152
Type	article
File Information	28saito.pdf



[Instructions for use](#)



Morphological and functional analyses of adult onset vitelliform macular dystrophy

W Saito, S Yamamoto, M Hayashi and K Ogata

Br. J. Ophthalmol. 2003;87;758-762
doi:10.1136/bjo.87.6.758

Updated information and services can be found at:
<http://bjo.bmj.com/cgi/content/full/87/6/758>

These include:

References

This article cites 15 articles, 3 of which can be accessed free at:
<http://bjo.bmj.com/cgi/content/full/87/6/758#BIBL>

Rapid responses

You can respond to this article at:
<http://bjo.bmj.com/cgi/eletter-submit/87/6/758>

Email alerting service

Receive free email alerts when new articles cite this article - sign up in the box at the top right corner of the article

Topic collections

Articles on similar topics can be found in the following collections

[Vision Research](#) (671 articles)
[Other ophthalmology](#) (2378 articles)

Notes

To order reprints of this article go to:
<http://www.bmjournals.com/cgi/reprintform>

To subscribe to *British Journal of Ophthalmology* go to:
<http://www.bmjournals.com/subscriptions/>

CLINICAL SCIENCE

Morphological and functional analyses of adult onset vitelliform macular dystrophy

W Saito, S Yamamoto, M Hayashi, K Ogata

Br J Ophthalmol 2003;**87**:758–762

Aim: To evaluate the morphology and visual function of the macula in eyes with adult onset vitelliform macular dystrophy (AVMD).

Methods: 12 eyes of six patients with AVMD were examined by ophthalmoscopy, scanning laser ophthalmoscopy (SLO), optical coherence tomography (OCT), and multifocal electroretinography (mfERGs). The macular lesions were bilateral in all patients and varied from the typical vitelliform (five eyes), faded vitelliform changes with retinal pigment epithelium (RPE) atrophy (five eyes), and a normal fovea associated with small flecks around the macula (two eyes).

Results: SLO demonstrated small abnormal bright spots in the deep retina throughout the posterior retina in all cases. OCT showed a highly reflective fusiform thickened layer at the level of the RPE and choriocapillaris in patients with a submacular yellow vitelliform lesion. A well circumscribed, optically clear space was observed beneath the retinal layer in the macular lesions with RPE atrophy. The mfERGs were significantly reduced not only in the macular area but also in the outermost ring (20–30°) of the mfERGs.

Conclusions: The submacular materials that accumulate within the RPE or subepithelial layers reported in previous histopathological studies of vitelliform lesions can be detected by OCT. In the macular lesions with RPE atrophy, the material may have disappeared leaving a subretinal or subepithelial optical clear space. These SLO and mfERG observations suggest that the morphological and functional abnormalities may not be localised just in the macular area but may be present throughout the posterior pole in eyes with AVMD.

See end of article for authors' affiliations

Correspondence to: Shuichi Yamamoto, MD, Department of Ophthalmology, Toho University Sakura Hospital, 564-1 Shimoshizu, Sakura, Chiba 2858741, Japan; shuyama@med.toho-u.ac.jp

Accepted for publication 9 October 2002

Adult onset vitelliform macular dystrophy (AVMD), first reported by Gass in 1974, is characterised by a yellow, solitary, round or oval subretinal macular lesion that resembles juvenile onset vitelliform macular dystrophy and Best's disease.¹ Other characteristics of AVMD include onset between ages 30 and 50 years, asymptomatic or mild decrease of visual acuity, and normal or subnormal electro-oculograms (EOGs).¹ Further studies showed that AVMD was a heterogeneous group of disorders displaying a variability in the size, shape, pigmentary changes, and distribution of the lesions.^{2–5} Clinicopathological studies showed a massive accumulation of lipofuscin pigments within the macular retinal pigment epithelium (RPE), and loss of the RPE and photoreceptor cell layer with infiltration of pigment containing macrophages in the central area.^{1–6,8}

The ophthalmoscopic appearance of the AVMD is very similar to that in Best's disease. Recently, the gene responsible for Best's disease, *VMD2*, has been identified as an RPE specific gene of 11 exons coding for a 585 amino acid protein of unknown function.^{9,10} Mutations in the *VMD2* gene have also

been found in some patients diagnosed with AVMD but not in patients with age related macular degeneration, suggesting a considerable overlap in the aetiology of AVMD and Best's disease.^{11–13} Another genetic study showed that a significant number of AVMD patients had a point mutation in the peripherin/RDS gene.¹⁴

Optical coherence tomography (OCT) gives a cross sectional image of the retina and provides information that is similar to that obtained from histological sections.¹⁵ We report the OCT determined macular configurations, and the multifocal electroretinogram (mfERG) determined macular function in six Japanese patients with AVMD.

PATIENTS AND METHODS

The clinical features of six patients with AVMD, seen at the eye clinic of Toho University Sakura Hospital, are summarised in Table 1. The patients' ages at the time of diagnosis ranged from 40 to 54 years. None of the patients had a family history of macular dystrophy. All patients underwent a complete

Table 1 Summary of patients' clinical characteristics and results of electrophysiological studies

Patient No	Age	Sex	Age of onset	VA		Macular appearance	
				RE	LE	RE	LE
1	40	M	39	20/30	20/20	Vitelliform	Vitelliform
2	51	F	50	20/20	20/20	Vitelliform	RPE atrophy
3	46	F	46	20/20	20/20	Vitelliform	RPE atrophy
4	52	M	51	20/25	20/20	Vitelliform	Flecks only
5	54	M	47	20/25	20/25	Faded vitelliform	Vitelliform
6	52	M	47	20/40	20/40	Faded vitelliform	Faded vitelliform

VA = visual acuity.

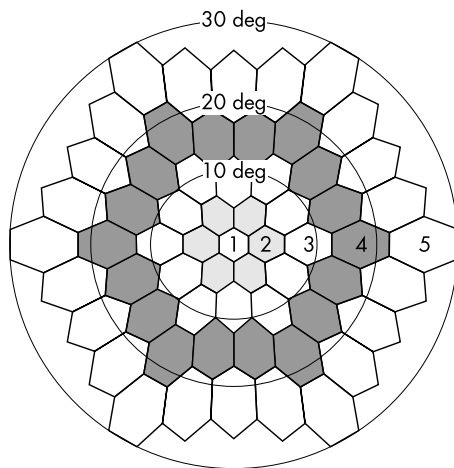


Figure 1 A diagram of the stimulus array for the mfERG recordings. Responses were grouped into five retinal eccentricities.

ophthalmic examination, including best corrected visual acuity measured with a Snellen chart, visual field testing with the Humphrey field analyser, indirect ophthalmoscopy, fluorescein angiography, indocyanine green angiography, scanning laser ophthalmoscopy (SLO), full field electroretinography (ERG) under photopic and scotopic conditions, mfERGs, and EOGs. The diagnostic criteria for AVMD were the presence of round or oval, solitary submacular yellow lesions in one or both eyes; onset between 30 and 50 years of age; normal or subnormal EOG light/dark ratio; and the ruling out of other macular diseases—for example, Best's disease, age related macular degeneration (by onset of symptoms), ophthalmoscopic findings, and fluorescein and indocyanine green angiograms. Blood samples have been drawn from all patients for molecular genetic analysis but the results are still not available.

This study followed the tenets of the Declaration of Helsinki. Informed consent was obtained from all subjects after the nature and possible consequences of the study had been explained.

Optical coherence tomography (OCT) was performed on all patients using the Humphrey model 2000 OCT (Humphrey Instruments, San Leandro, CA, USA). The patient's pupil was fully dilated with topical 0.5% tropicamide and 0.5% phenyl-

ephrine hydrochloride, and the fundus was scanned with a probe beam positioned so that the horizontal and vertical scans crossed the central fovea as determined from fundus photographs. The scan length was usually 2.8 mm.

MfERGs were recorded with the Visual Evoked Response Imaging System (VERIS science, EDI, San Mateo, CA, USA). The stimulus matrix consisted of 61 hexagons that were arranged concentrically and covered approximately 50 degrees of the central visual field. The size of each hexagon was scaled to give approximately equal ERG responses from normal eyes. Each hexagon was independently alternated between black and white according to a pseudorandom binary m-sequence at a rate of 75 Hz. A Burian-Allen bipolar contact lens electrode was used for the recordings, and a ground electrode was placed on the earlobe. The patient's pupil was fully dilated with topical 0.5% tropicamide, and the opposite eye was occluded. After the patients had undergone optical correction for a viewing distance of 30 cm, they were instructed to maintain their fixation on the fixation spot. The signals were amplified 100 000 times with a bandpass filter of 10–300 Hz. The recording period was composed of eight segments of 30 seconds, providing a total recording time of 4 minutes.

To evaluate spatial differences in the electrical responses, the 61 hexagonal elements were divided into five concentric rings around the fovea as shown in Figure 1. The amplitude of the positive component was measured, and the response density (nV/deg^2) was calculated by dividing the response amplitude (nV) by the retinal area (deg^2). The data from the patients were compared with those from 21 age similar normal subjects (38–60 years of age).

RESULTS

Ophthalmoscopic appearance

The ophthalmoscopic findings of six AVMD patients are summarised in Table 1. A vitelliform-like macular lesion was observed in six eyes of five patients. In patient 1, the vitelliform-like lesion was bilateral. In patient 2, there was a subretinal yellow lesion in the right macula (Fig 2A), and a round lesion with RPE atrophy surrounded by a hypopigmented ring in the left macula (Fig 2B). In patient 4, a vitelliform macular lesion with multiple flecks was observed in the right eye; however, only small yellow flecks were observed around the left macula. A faded vitelliform macular lesion associated with RPE atrophy was observed in the right eye of patient 5 (Fig 3A) and in both eyes of patient 6 (Fig 4A, 4B).

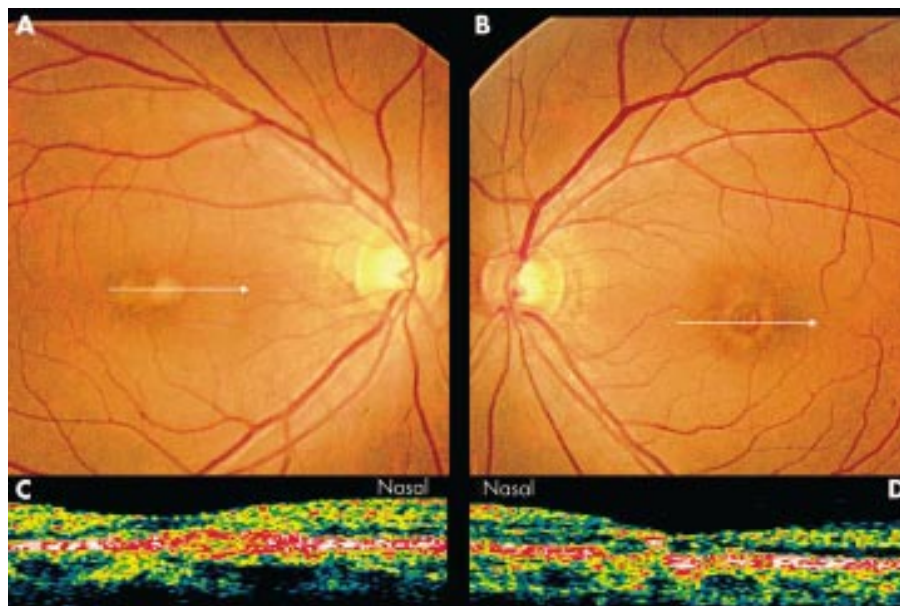


Figure 2 Patient 2. Ophthalmoscopic appearance of the right eye (A) with a vitelliform lesions and left eye (B) with the RPE atrophy surrounded by a yellow ring. OCT images through the fovea show a highly reflective, well circumscribed elevation of the retinal pigment epithelium in the right eye (C), and irregularity of the highly reflective layer of the retinal pigment epithelium in the left eye (D). White arrows on the fundus photographs indicate the region scanned by OCT (A, B).

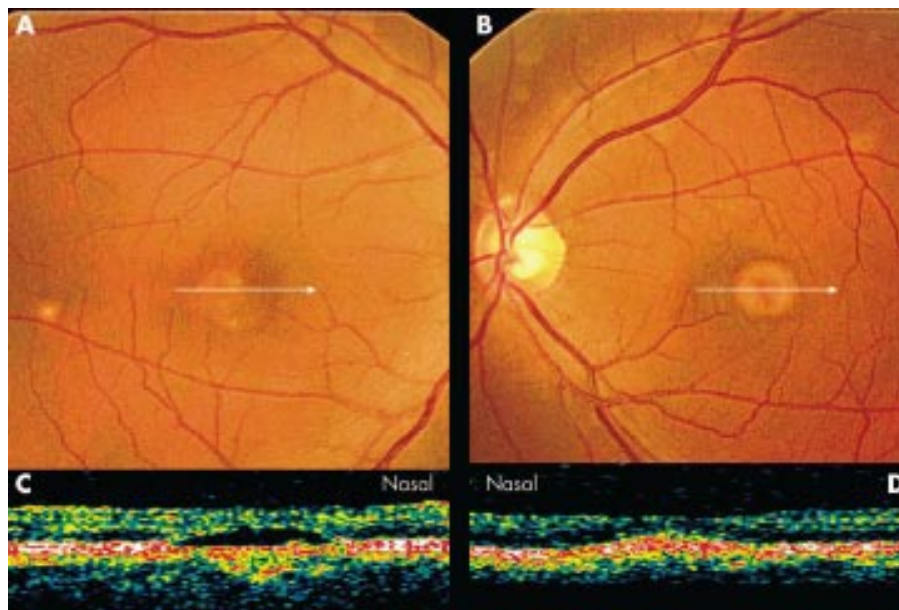


Figure 3 Patient 5. Ophthalmoscopic appearance of the right eye (A) with faded vitelliform changes and the RPE atrophy and left eye (B) with a vitelliform lesion. OCT images show an optical clear space beneath the retinal layer in the right eye (C), and a highly reflective elevation of the retinal pigment epithelium in the left eye (D).

Fluorescein angiography showed hypofluorescence at the centre of the vitelliform lesion with a marginal hyperfluorescent ring from the early phase to the late phase. There was no evidence of a dark choroid and choroidal neovascularisation. Hyperfluorescence due to window defects was observed in the vitelliform faded lesions and the RPE atrophy lesions.

Fundus examination with the SLO and infrared diode laser revealed small bright spots throughout the posterior pole in all eyes with a vitelliform macular lesion (Fig 5).

OCT images

The OCT images acquired through the yellow macular lesions showed a highly reflective, well circumscribed elevation of the retinal pigment epithelium above a moderately reflective region in all eyes (Fig 2C, 3D). The retinal layers above the lesion appeared compressed. The OCT images through the macular areas without a vitelliform lesion or RPE degeneration showed normal foveal contours (Fig 2D). The macular lesions associated with partially faded vitelliform changes appeared as a low reflecting, well circumscribed space beneath

the retinal layer, resembling an accumulation of subretinal fluid. The layer beneath the optical clear space was less reflective than the normal RPE and choriocapillaris (Fig 3C, 4C, 4D).

MfERGs

The 61 local responses of mfERGs (top) and the three dimensional plot of the amplitudes of the mfERGs (bottom) recorded from the right eye of a normal subject and a patient with AVMD (patient 2) are shown in Figure 6. The mfERG consisted of a negative wave followed by a positive wave, and these waves have been shown to correspond to the a-waves and b-waves, respectively, of the conventional cone ERG to flash stimuli.¹⁶

In the AVMD patient, the responses from the central retina were severely depressed compared with those in normal controls. The response density of the positive component of the mfERGs from ring 1 (macular response) and ring 5 (most outer ring, 20–30 degrees) are summarised for all eyes in Table 2. The macular response was within the normal range in only one eye (patient 2, left eye). The mean (SD) of the electrical

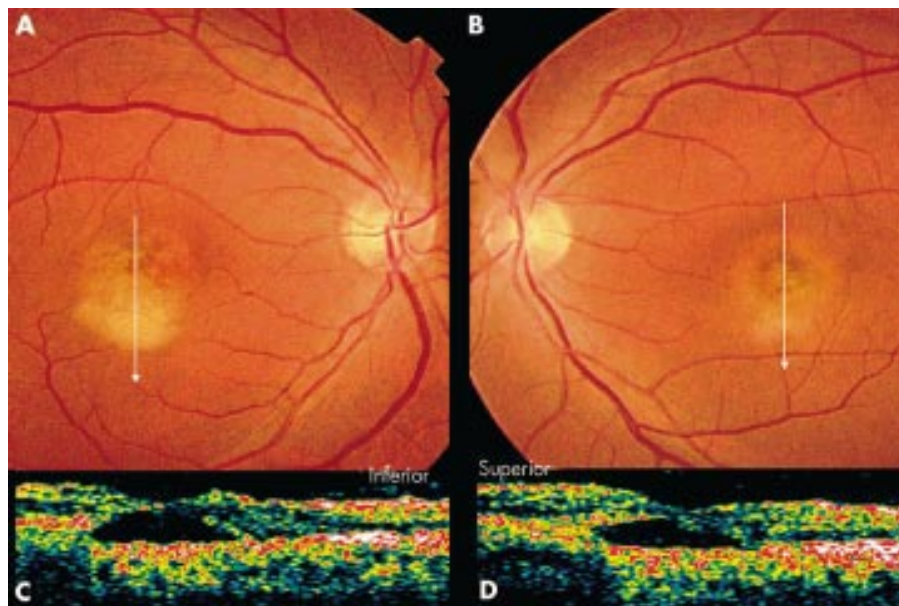


Figure 4 Patient 6. Ophthalmoscopic appearance of the right (A) and left eye (B) with a combination of vitelliform changes and the RPE atrophy. OCT images show an optical clear space accompanied by a moderately reflective region beneath the retinal layer in the right (C) and left eyes (D).

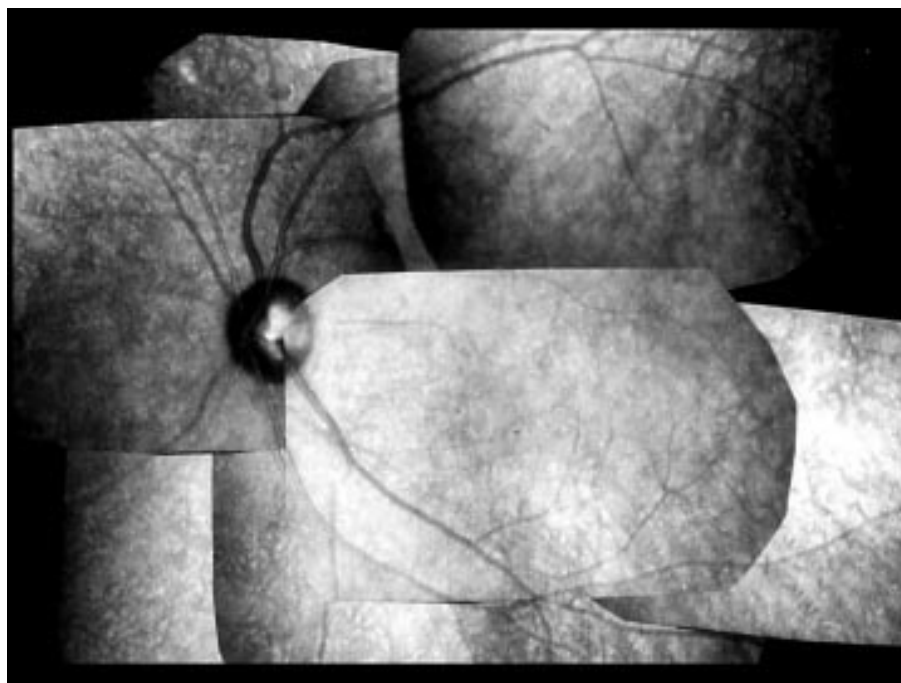


Figure 5 Patient 4. Scanning laser ophthalmoscopic appearance obtained by an infrared diode laser revealing small bright spots throughout the posterior pole.

macular response was 32.8 (13.3) nV/deg² in AVMD patients, and 64.2 (12.2) nV/deg² in normal subjects, and this difference was statistically significant ($p < 0.0001$, unpaired t test). The response density in ring 5 was also significantly reduced in AVMD patients (11.9 (2.9) nV/deg²) compared to that in normal subjects (15.5 (3.8) nV/deg²; $p = 0.008$, unpaired t test). No significant difference was observed in the implicit times in rings 1 and 5 between AVMD patients and normal subjects.

Both cone and rod ERGs to full field flash stimuli were normal in all patients. The light/dark ratios of the EOG were below the normal range for the right eye of patient 1, and for both eyes in patients 3 and 6 (Table 2).

DISCUSSION

Gass originally described the AVMD lesions as bilateral, symmetrical, solitary, usually one third to one disc diameter in

size, round or oval, slightly elevated, yellowish, subretinal lesions, often with a central pigmented spot.¹ With over 100 cases reported since then, the ophthalmoscopic criteria have been expanded and the presence of a central grey or orange pigment spot, fading of the yellow materials, and additional atrophic changes of the RPE have become optional diagnostic criteria.²⁻⁵ In our series of AVMD patients, all cases showed bilateral macular lesions, which varied in appearance from the typical round yellow subretinal lesion to RPE atrophy, or to normal fovea with multiple satellite flecks, as have been reported previously.

The OCT images through the macular lesions in two AVMD patients were first demonstrated by Puliafito and associates.¹⁷ The OCT images in our six patients had different macular appearances corresponding to their ophthalmoscopic appearance. Because there have been only a few histopathological

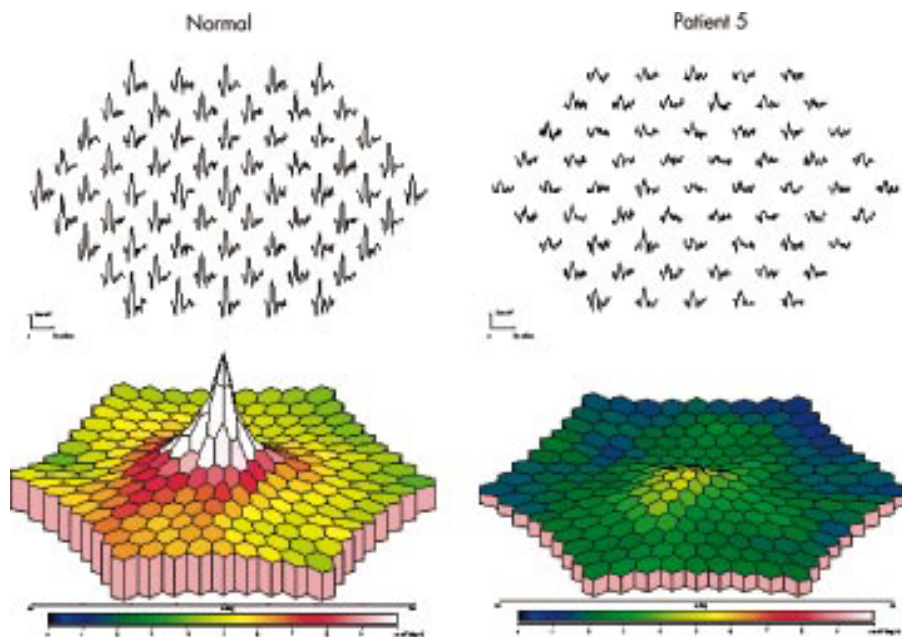


Figure 6 Trace array of 61 local responses of mfERGs (top) and 3D plot of the amplitudes of the mfERGs (bottom) recorded from the right eye of a normal subject and a patient with AVMD. The calibration markers represent 200 nV vertically and 80 ms horizontally.

Table 2 Results of electrophysiological studies

Patient No	mfERG amplitude (RE/LE, nV/deg ²)		EOG L/D ratio (RE/LE)
	Ring 1	Ring 5	
1	33.6/46.0	18.0/15.7	1.51/1.81
2	57.2/30.9	13.8/10.1	2.20/2.20
3	48.5/37.4	11.3/13.0	1.71/1.53
4	29.7/35.5	9.4/12.2	2.62/2.57
5	20.3/26.0	11.1/8.2	1.85/1.91
6	11.8/17.0	8.6/10.9	1.46/1.38
Normal range (n=21)	50.8–98.7	9.6–25.5	>1.85

EOG = electro-oculogram; L/D ratio = light/dark ratio.

cases of AVMD reported,^{1–6,8} and because OCT images depict only the differences of reflectivity of the tissue, the exact interpretation of the OCT findings is difficult. In the case described by Gass,¹ a slightly elevated, round, yellow subretinal lesion with a central pigmented spot was observed ophthalmoscopically. Histopathologically there was focal loss of the photoreceptor nuclei with loss of inner and outer segments and atrophy of the subjacent RPE in the fovea. A large clump of extracellular pigment in the foveal area corresponding to the central pigment spot ophthalmoscopically was also reported. Patrinely *et al*⁶ presented a clinicopathological report on an AVMD patient showing a partially faded vitelliform lesion with RPE atrophy and described atrophy of the photoreceptors and RPE. In both reports, dense eosinophilic materials were observed between Bruch's membrane and the RPE.

Jaffe and Schatz⁷ studied a case of AVMD with a macular lesion of the central area of hyperpigmentation with a surrounding yellowish rim, and reported that the sensory retina was detached by pale eosinophilic fluid, and the RPE was also detached by periodic acid Schiff (PAS) positive fluid. Dubovy *et al*⁸ reported the clinicopathological studies on three patients with AVMD. In their first patient with a circular retinal pigment epithelial atrophy, they observed a marked central loss of photoreceptors, mild retinal pigment epithelial atrophy, and basal laminar deposits. Their second patient with a vitelliform lesion showed atrophy of the RPE, a thin layer of subretinal pigment epithelial material, and pigment containing cells that contained PAS positive materials in the subretinal space. The third patient with vitelliform lesion had a loss of the RPE, atrophy of photoreceptors, and pigmented cells containing lipofuscin in the subfoveal space.

In this study, the OCT images acquired through the yellow vitelliform lesions demonstrated a well circumscribed elevation of the RPE layer above a moderately or highly reflective region. This finding probably corresponds to a clump of the RPE, subretinal pigment epithelial material, pigment cells containing PAS positive materials, and/or thickened Bruch's membrane. The atrophy of photoreceptor was also seen as a thinning of the retinal layer in the OCT images.

In the macular lesions where the vitelliform changes faded with atrophy of the RPE, the OCT images showed a well circumscribed non-reflective region, suggesting a serous retinal detachment or a serous pigment epithelial detachment. Interestingly, these OCT images showed a striking resemblance to the light microscopic sections in the first patient of Dubovy *et al*'s series.⁸ Therefore, this optically clear region can be considered to represent a loss of photoreceptors and/or accumulation of eosinophilic fluid as was reported by Jaffe and Schatz.⁷ OCT images through the fovea that appeared normal ophthalmoscopically showed a normal foveal contour without thinning of the photoreceptor layer (patient 1, left eye and patient 4, left eye). Further clinicopathological studies combined with the OCT imaging will be needed to interpret the OCT images more definitively.

The mfERGs were markedly reduced in all eyes except the right eye of patient 2. Interestingly, the amplitude of the central response was below the normal limits in eyes with normal visual acuity, and even in eyes with normal macula such as the left eyes of patients 1 and 4. These findings would indicate that the visual function in the macular area was far more impaired than the visual acuity in AVMD patients. Furthermore, the electrical responses from the outermost ring were also significantly reduced compared with those in normal subjects, showing that the visual function was affected not only in the macular area but also in the more peripheral retina. These electrophysiological findings support the observations by the SLO that abnormalities at the RPE level were not localised in the macular region but spread throughout the posterior pole.

In summary, our findings demonstrated that the OCT determined cross sectional images of the macular lesions in six patients with AVMD corresponded well with the different ophthalmoscopic appearances. Because the OCT images could also be correlated with the previously reported histopathological findings, a better understanding of the ophthalmoscopic appearance of the macula was obtained. The SLO and the mfERG results indicated widespread abnormalities in the deep retina throughout the posterior pole. Further studies of the morphology and visual functions combined with genetic analyses will be necessary to clarify the pathogenesis of AVMD, and reconcile the relation between AVMD, Best's disease, and age related macular degeneration.

Authors' affiliations

W Saito, S Yamamoto, M Hayashi, K Ogata, Department of Ophthalmology, Toho University Sakura Hospital, Sakura, Japan

REFERENCES

- Gass JDM. A clinicopathologic study of a peculiar foveomacular dystrophy. *Trans Am Ophthalmol Soc* 1974;**72**:139–56.
- Kingham JD, Lochen GP. Vitelliform macular degeneration. *Am J Ophthalmol* 1977;**84**:526–31.
- Vine AK, Schatz H. Adult-onset foveomacular pigment epithelial dystrophy. *Am J Ophthalmol* 1980;**89**:680–91.
- Epstein GA, Rabb MF. Adult vitelliform macular degeneration: diagnosis and natural history. *Br J Ophthalmol* 1980;**64**:733–40.
- Gass JDM. Dominantly inherited adult form of vitelliform foveomacular dystrophy. In: Fine SL, Owens SL, eds. *Management of retinal vascular and macular disorders*. Baltimore: Williams and Wilkins, 1983:182–6.
- Patrinely JR, Lewis RA, Font RL. Foveomacular vitelliform dystrophy, adult type: a clinicopathologic study including electron microscopic observations. *Ophthalmology* 1985;**92**:1712–18.
- Jaffe GJ, Schatz H. Histopathologic features of adult-onset foveomacular pigment epithelial dystrophy. *Arch Ophthalmol* 1988;**106**:958–60.
- Dubovy SR, Hairston RJ, Schatz H, *et al*. Adult-onset foveomacular pigment epithelial dystrophy: clinicopathologic correlation of three cases. *Retina* 2000;**20**:638–49.
- Marquardt A, Stohr H, Passmore LA, *et al*. Mutations in novel gene, VMD2, encoding a protein of unknown properties cause juvenile-onset vitelliform macular dystrophy (Best's disease). *Hum Mol Genet* 1998;**7**:1517–25.
- Petrukhin K, Koisti MJ, Bakall B, *et al*. Identification of the gene responsible for Best macular dystrophy. *Nat Genet* 1998;**19**:241–7.
- Allikmets R, Seddon JM, Bernstein PS, *et al*. Evaluation of the Best disease gene in patients with age-related macular degeneration and other maculopathies. *Hum Genet* 1999;**104**:449–53.
- Kramer F, White K, Pauleikhoff D, *et al*. Mutations in the VMD2 gene are associated with juvenile-onset vitelliform macular dystrophy (Best disease) and adult vitelliform macular dystrophy but not age-related macular degeneration. *Eur J Hum Genet* 2000;**8**:286–92.
- White K, Marquardt A, Weber BHE. VMD2 mutation in vitelliform macular dystrophy (Best disease) and other maculopathies. *Hum Mutat* 2000;**15**:301–8.
- Felbor U, Schilling H, Weber BHE. Adult vitelliform macular dystrophy is frequently associated with mutations in the peripherin/RDS gene. *Hum Mutat* 1997;**10**:301–9.
- Toth CA, Narayan DG, Boppart SA, *et al*. A comparison of retinal morphology viewed by optical coherence tomography and by light microscopy. *Arch Ophthalmol* 1997;**115**:1425–8.
- Hood DC, Seiple W, Holopigian K, *et al*. A comparison of the components of the multifocal and full-field ERGs. *Vis Neurosci* 1997;**14**:533–44.
- Puliafito CA, Hee MR, Schuman JS, *et al*. *Optical coherence tomography of ocular disease*. Thorofare, NJ: Slack, 1996:269–73.